Journal of The Electrochemical Society, **158** (12) A1313-A1319 (2011)
0013-4651/2011/158(12)/A1313/7/$28.00 © The Electrochemical Society

Influence of Two-Step Heat Treatment on Sputtered Lithium Cobalt Oxide Thin Films

Y. S. Yoon,[a] S. H. Lee,[a] S. B. Cho,[b] and S. C. Nam[c,z]

[a]*Department of Materials Science and Engineering, Yonsei University, Seoul 120-749, Korea*
[b] *Advanced Technology Research Center, Agency for Defense Development, Yuseong, Daejeon 305-600, Korea*
[c]*GS Nanotech Co. Ltd., Gangdong-gu, Seoul 134-848, Korea*

A crack-free $LiCoO_2$ thin film with a preferred oriented crystalline structure is obtained by adopting a two-step heat treatment with a combination of substrate heating at 300°C during sputtering and a rapid thermal annealing (RTA) process. The performances of cells deposited at room temperature and at 600°C with and without the RTA process are also compared. The $LiCoO_2$ cathode thin film deposited at 300°C with RTA shows a high specific discharge capacity of 65 $\mu Ah/cm^2$-μm at a 1C rate and excellent reversibility of the dQ/dV curve in a half cell using liquid electrolyte. In a Li/Lipon/$LiCoO_2$ structure, a specific discharge capacity of 63.5 $\mu Ah/cm^2$-μm is demonstrated, corresponding to 92% of its theoretical value. During charge and discharge the first specific discharge capacity of 60 $\mu Ah/cm^2$-μm is observed even at a 5 C rate, demonstrating superior cycling performance over 500 cycles with no capacity degradation.
 [DOI: 10.1149/2.036112jes]

Manuscript submitted June 28, 2011; revised manuscript received September 2, 2011. Published November 1, 2011.

Lithium rechargeable thin film batteries comprising solid state components, especially a solid electrolyte, are promising power sources in novel electronic devices such as MEMS, smart cards, sensors and healthcare due to their advantages of safety, wide operating temperatures, very low self discharge and long cycle life.[1–4] Additionally, the batteries are gradually expanding to use in application fields, such as autonomous micropower supply, through combination with energy harvesting devices. There are various transition metal oxide compounds to capitalize on the intercalating capability of lithium ions in lithium ion batteries. Among them, lithium cobalt oxide ($LiCoO_2$) with a layered rock salt structure has been widely studied, especially in thin film batteries using a vacuum process, such as physical vapor deposition (PVD), because of easy control of the film composition, excellent charge/discharge reversibility after crystallization, a high operating potential of ~4.0 V (vs. Li/Li^+) and a reversible theoretical capacity of 69 $\mu Ah/cm^2$-μm over the range of $0.5 \leq x \leq 1$ in Li_xCoO_2.[5–13] However, most of the $LiCoO_2$ thin films deposited at room temperature or relatively low temperatures below 600°C lacked crystallinity. In order to produce a battery with high capacity and cycleability based on reversible lithium insertion and extraction, high crystallinity is required, which can be achieved using an optimal heat treatment process.[14] For crystallization of $LiCoO_2$ thin film, direct heat treatment of the thin film surface in a furnace is one of the simplest and most economical processes. Unfortunately, heat treatment conducted using a conventional furnace or rapid thermal annealing (RTA) process at high temperatures greater than 700°C is likely to cause film cracks and voids due to differences in the thermal expansion coefficients between the $LiCoO_2$ thin film and the substrate. These drawbacks were already reported by previous works and could cause micro-short path when the solid electrolyte and lithium anode were deposited, subsequently.[15,16] These phenomena can be regarded as a critical factor to decrease the long term cycling stability of thin film batteries. In general, a lower process temperature reduces such problems. However, insufficient heat treatment produces a low temperature (LT) phase of $LiCoO_2$ thin film, resulting in poor cycleability, low rate capability and high self discharge rate.[17] In spite of that, crystallization through heat treatment is regarded as one of the most useful methods to date. Heating a substrate during deposition is very effective for producing an optimal crystallinity in the as-grown $LiCoO_2$ thin film. But, this process involves high cost or a complex system geometry and is not suitable for use as a continuous process. Although the effect of ion bombardment due to application of a bias to the substrate was reported to minimize crack formation during crystallization in the sputtering method, it is important to maintain the low deposition rate of re-sputtering and the relatively low reversibility.[15] Another heat treatment method is to crystallize the $LiCoO_2$ thin film within very short time using rapid thermal annealing (RTA) process, but there still exist crack formation.[16] In this present study, we propose a method to fabricate crack-free thin films of $LiCoO_2$ preventing the formation of a micro-short path through a two-step heat treatment by substrate heating during deposition and rapid thermal annealing after deposition. The resulting effectiveness and performance enhancement are also discussed. To the best of our knowledge, crack-free $LiCoO_2$ thin films after heat treatment have not been previously reported.

Experimental

$LiCoO_2$ thin films were deposited on a 500-μm-thick alumina substrate (Coors, USA) using radio frequency (RF) magnetron sputtering (Anelva, Japan) with an applied power density of 2.5 W/cm^2 under an Ar gas condition. Layers of Ti (30 nm) / TiO_2 (25 nm) / Pt (250 nm) / $LiCoO_2$ (700 nm) were consecutively deposited over an electrode area of 3.6 cm^2. Titanium and titanium oxide were inserted between the substrate and a Pt current collector to improve the adhesion and minimize the interlayer diffusion during deposition, respectively. The round sintered sputtering target (4 inches in diameter) was fabricated using $LiCoO_2$ powder (battery grade, Seimi), which was calcined at 500°C, followed by ball milling for 24 h. A polyvinyl alcohol (PVA) binder (2 wt%) was added to the powder, and the resulting powder was pelletized under a pressure of 100 kgf/cm^2 before sintering at 1000°C for 3 h. Before deposition, the target was pre-sputtered for 30 min to eliminate the surface contamination after chamber evacuation to 2.7×10^{-4} Pa. The Ar gas pressure during deposition was maintained at 1.7 Pa with an 120 mm distance from the target to the substrate for minimizing the temperature elevation of the substrate during sputtering.

The substrate temperature was controlled at room temperature (RT), 300°C and 600°C to compare the crack formations. As a second heat treatment, RTA (Atech system, Korea) was used in a separate vacuum chamber maintained at atmospheric pressure via purging of Ar gas, wherein halogen lamps were used as a heating source. The temperature ramping rate was approximately 63°C/min to 650°C for 10 min. The molar ratio (Li/Co) and crystallinity of the $LiCoO_2$ thin film were analyzed using an inductively coupled plasma (ICP, Thermojarrell ASH, Polyscan 61E) and an X-ray diffractometer (XRD, Rigaku) using CuKα radiation, respectively. The surface morphologies of the $LiCoO_2$ thin films were observed using scanning electron microscopy (SEM, Hitachi S-4100) to analyze crack formation during deposition onto heated substrates and after the RTA process. The

[z] E-mail: scnam@gsnanotech.co.kr

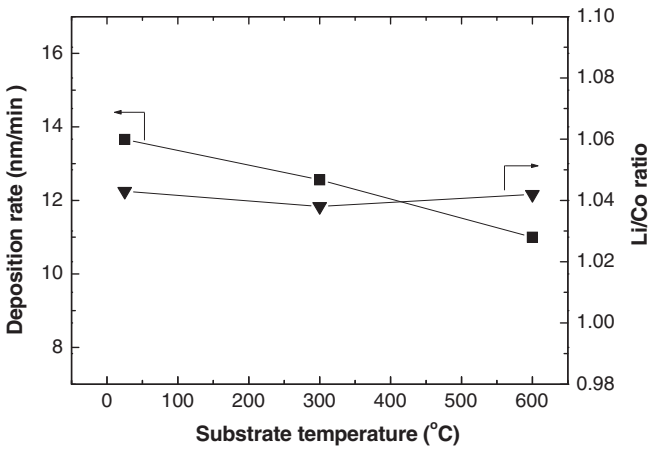

Figure 1. Deposition rate and molar ratio of Li/Co in $LiCoO_2$ thin films at various substrate heating temperatures.

half-cells were assembled with lithium foil (FMC) as a counter electrode and 1 M $LiPF_6$ in EC:DMC (1:1, Merck) as an electrolytic solution with a polyethylene separator (Ube). To fabricate all-solid-state batteries, lithium phosphorous oxynitride (Lipon) with a 1.5 μm thickness and lithium with a 2 μm thickness were employed as the solid electrolyte and anode, respectively. Lipon was deposited onto the $LiCoO_2$ surface using RF reactive sputtering under pure nitrogen gas using a Li_3PO_4 target in the same chamber, and a lithium thin film was deposited in a glove box (dew point: -80°C) using a thermal evaporator. The charge-discharge profile was obtained using a constant current battery cycler system (WBCS3000, Won-A Tech.) connected to a glove box in the range of 3.0 V–4.2 V.

Results and Discussion

In general, the crystalline phase and stoichiometry of $LiCoO_2$ are regarded as critical factors for determining cell capacity and reversible cycleability. When the molar ratio of Li/Co exceeds 1, the material is likely to form an unstable second phase, which can interfere with the movement of lithium ions and is sensitive to moisture in the as-deposited thin film. Alternatively, capacity decay likely occurs due to the formation of Co_3O_4 caused by lithium deficiency when the molar ratio of Li/Co is less than 1.[18] Figure 1 shows the deposition rate and molar ratio of Li/Co with substrate heating temperature. The average deposition rate measured using an alpha-step 500 profilometer was 13.7 nm/min at room temperature, which linearly decreased as the substrate temperature increased, resulting in an 11 nm/min deposition at 600°C. The desorption rate of absorbed atoms impinging on the substrate surface decreased at a low substrate temperature since the substrate temperature determines the mobility of atoms on the surface.[19] However, the atomic ratio of Li/Co in the present study did not change with an increase in the substrate temperature. When a mixture of Ar and O_2 was used as the working gas, negative oxygen ions in the plasma state can re-sputter the unstable and pre-rearranged $LiCoO_2$ thin film. Therefore, Li atoms of relatively low atomic weight could be removed from the substrate, resulting in a Li deficiency. Thus, the ratio of Li/Co was not affected under these conditions, although it did varied with substrate temperature at a fixed working pressure, especially under a condition of pure Ar working gas. This phenomenon was in good agreement with previous results that demonstrated the atomic ratio of Li/Co was constant at various substrate temperatures, while the ratio varied with process gas pressure.[18,20,21] Figure 2 shows

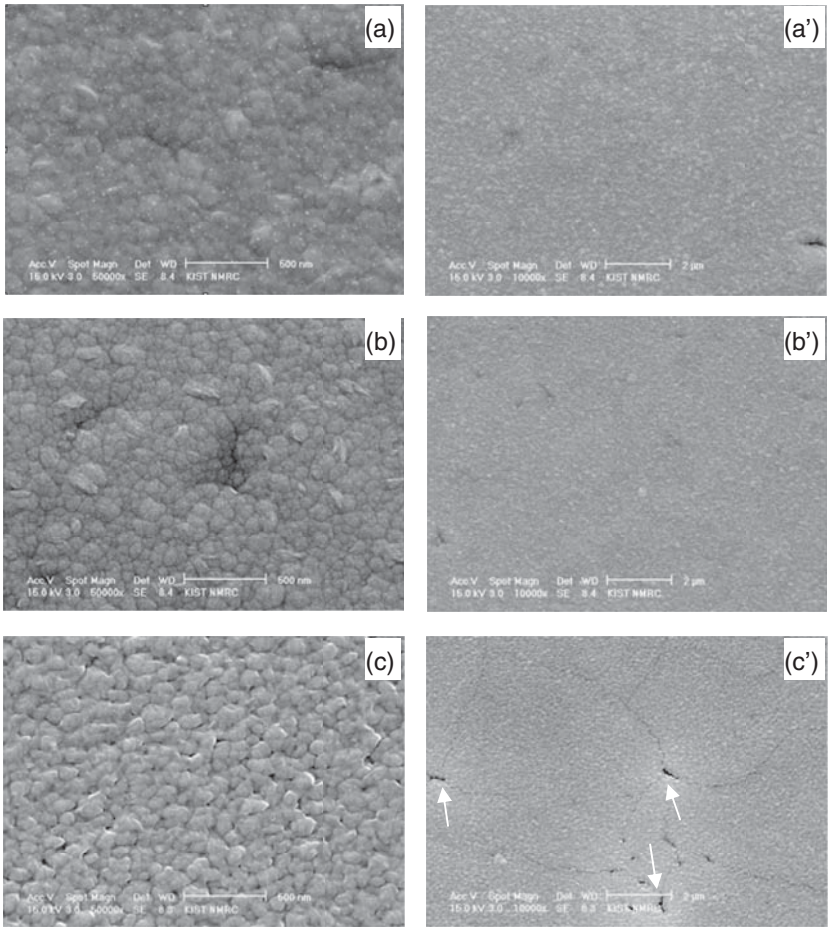

Figure 2. SEM images for $LiCoO_2$ thin film surfaces deposited at different substrate temperatures: (a),(a′) deposition at room temperature (×50,000, ×10,000), (b),(b′) deposition at 300°C (×50,000, ×10,000) and (c),(c′) deposition at 600°C(×50,000, ×10,000).

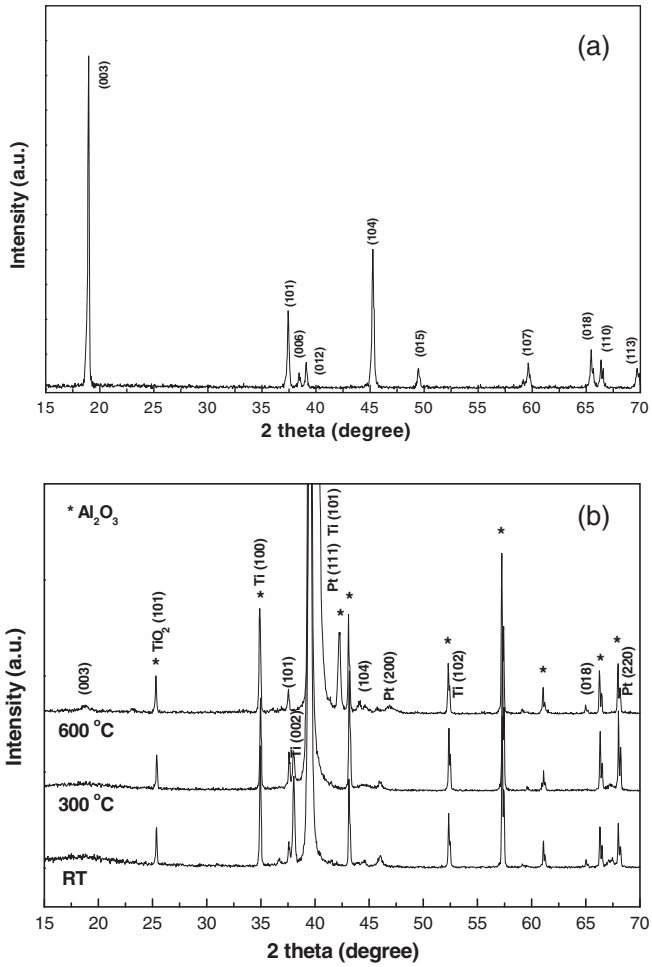

Figure 3. X-ray diffraction patterns of (a) $LiCoO_2$ target and (b) $LiCoO_2$ thin films with various substrate heating temperatures.

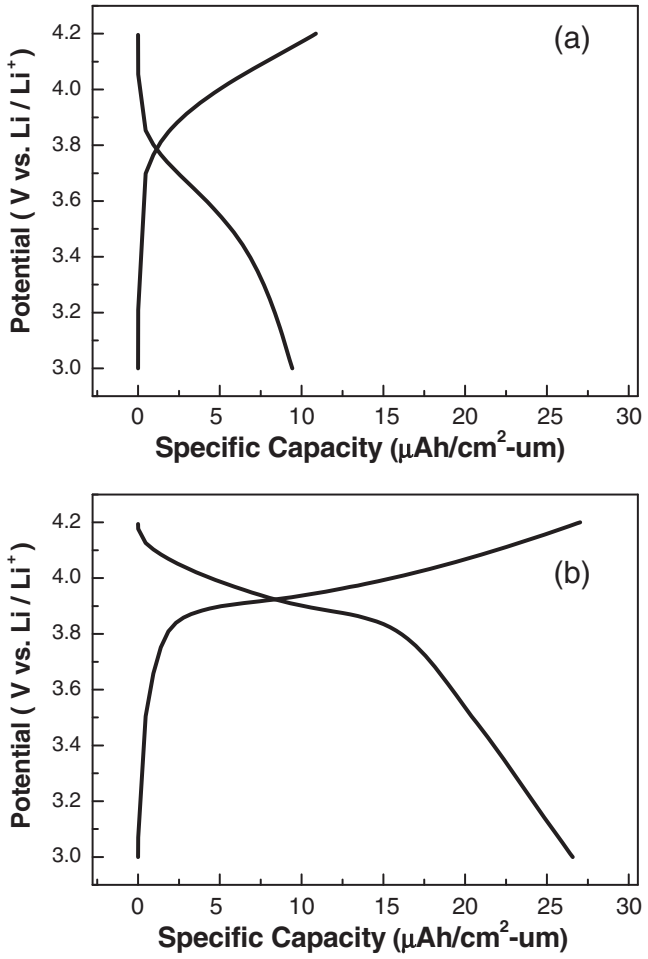

Figure 4. Charge-discharge curves of $LiCoO_2$ thin film in half cell test: (a) deposition at 300°C and (b) deposition at 600°C.

SEM images of $LiCoO_2$ thin film surfaces deposited at different substrate temperatures. As shown in Fig. 2a, a relatively smooth surface was obtained in a thin film deposited at room temperature, while the 80–90-nm-sized clusters consisted of fine 10-20-nm-sized grains grown at a 300°C deposition (Fig. 2b). However, an increasingly rough surface and some void fractions were observed at a high substrate temperature of 600°C and the cluster sizes increased to 100–120 nm, as shown in Fig. 2c. These phenomena are likely caused by high mobility of sputtered ad-atoms on the substrate as the temperature of the substrate was increased. As a result, grain growth occurred and large clusters developed both of which can affect the crystalline growth and increase the possibility of lithium intercalation. As shown in the low magnification SEM images, the crack-free $LiCoO_2$ thin films were obtained at RT and 300°C deposition, respectively (Fig. 2a′ and 2b′); however, critical defects at several spots were observed in the sample deposited at 600°C (Fig. 2c′). Some defects generated along the fine cracks were attributed to film shrinkage induced by excessive thermal stress during high temperature deposition. The diffraction patterns of thin films deposited at RT and with a heated substrate were analyzed using XRD and were compared to that of the sputtering target. As shown in Fig. 3a, a typical hexagonal $R\bar{3}m$ polycrystalline structure of HT-$LiCoO_2$ consisting of an edge-shared oxygen tetrahedron was measured in the sputtering target, while the low peak intensity corresponding to the (101), (018) planes near 37° and 65° and another broad peak near 18.5° were observed on the film deposited at RT. It is notable that the peaks of the (003) plane of the (104) plane near 45° were shown in the film deposited at 600°C, while the peak intensity of the (101) plane slightly increased at 300°C. Therefore, the increase in substrate temperature affected the texturing of the (003), (104) and (018) planes, but not that of the (101) plane, due to atomic rearrangement via thermal energy. As a result, the poly-crystallinity of $LiCoO_2$ increased with an increase in the substrate temperature during deposition. The peak shifts of the (104) and (018) planes to lower 2Θ were due to not ideal lattice occupations of the atoms. Similarly, Iriyama et al. reported that randomly oriented polycrystalline $LiCoO_2$ thin film having (101), (012) and (104) peaks was obtained at thicknesses greater than 340 nm in a thin film deposited at 600°C using pulsed laser deposition (PLD), while only the c-axis-oriented peaks were detected at thicknesses less than 240 nm.[22] Pelleg et al. reported that the volume strain energy was dominant in a thin film thicker than 1 μm, and Hart et al. reported that the volume strain energy densities of the (101) and (104) planes in a lattice model of $LiCoO_2$ were quite small compared to that of the (003) plane.[23,24] Therefore, the diffraction peaks of 700-nm-thick $LiCoO_2$ thin films were developed to minimize the volume strain energy. The crystal phase of $LiCoO_2$ was divided into a high temperature (HT) phase of the hexagonal structure and a low temperature phase (LT) of a cubic-spinel related structure for different spatial arrangement of cations, although it had the same oxide sublattice.[25] In terms of battery performance, the HT phase was beneficial for power and charge-discharge cycling. However, as shown in Fig. 3b, peak separation of the (018) and (110) planes near 65° did not occur, which indicates the formation of a LT phase, as reported by Gummow et al.[26] With regard to the crystal structure, the (101) and (104) textures were preferable because the (003) plane in the direction parallel to the substrate was hindered for easy diffusion of Li ions.[7] Figures 4a and 4b show the charge and discharge potential curves, measured at a 1 C

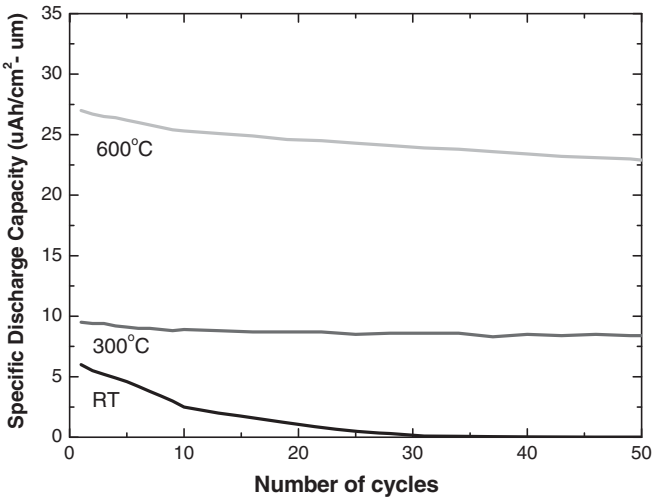

Figure 5. Cycling performances of $LiCoO_2$ thin films at a 1 C rate with various substrate heating temperatures.

rate (current density of 48 uA/cm^2), of $LiCoO_2$ thin films deposited at 300°C and 600°C, respectively. As shown in Fig. 4a, the rapid voltage decrease of as much as 0.4 V was measured with no potential plateau in a $LiCoO_2$ thin film at 300°C. The first specific discharge capacity was only 9.5 μAh/cm^2-μm. In contrast, the potential decrease was reduced significantly, and a plateau region over the potential range of approximately 3.8 V–3.9 V was shown on the film deposited at 600°C (Fig. 4b). However, in this case, a low specific discharge capacity of 27 μAh/cm^2-μm corresponding to approximately 39% of the theoretical value, indicates poor electrode characteristics. In a typical LT-$LiCoO_2$ phase, a short plateau near 3.8 V, a long plateau near 3.5 V and a large cell polarization are observed.[27] Instead, prolonged potential profiles were observed in both cases in the present study. Therefore, it is estimated that the $LiCoO_2$ thin films deposited with substrate heating existed as an HT and LT mixed phase, the ratio of which was greater at 600°C. Cycling behaviors of $LiCoO_2$ thin films with different substrate heating temperatures were conducted at a 1C rate. As shown in Fig. 5, the specific discharge capacity retention of $LiCoO_2$ thin films deposited at 300°C and 600°C were approximately 88% and 85% after 50 cycles, respectively, while the initial specific discharge capacity rapidly dropped from 6 μAh/cm^2-μm to 2.5 μAh/cm^2-μm within ten cycles at RT deposition. Increasing only the substrate temperature during deposition resulted in the formation of an LT phase of $LiCoO_2$ with a relatively low capacity and poor cycling behavior. Although the data was not included in this article, the self discharge rate in a charging state was high. Therefore, an increase in substrate heating temperature above 600°C is required to improve the crystallinity of $LiCoO_2$ thin film in order to produce a higher capacity. However, prolonged deposition is needed in order to obtain the desired film thickness as the substrate heating temperature increases. Thus, it is not desirable as it cause inter-diffusion between the cathode and current collector during the deposition process, which can increase the interface resistance between the cathode and current collector to produce a lower cell capacity. When the substrate heating temperature exceeds the 600°C, film delamination may occur. Because the preferred (101) and (104) planes are favorable for easy diffusion of lithium ions in all-solid-state thin film batteries, the additional RTA process minimizing the inter-diffusion between the cathode and current collector is necessary. As shown in Fig. 6a, severe cracks with

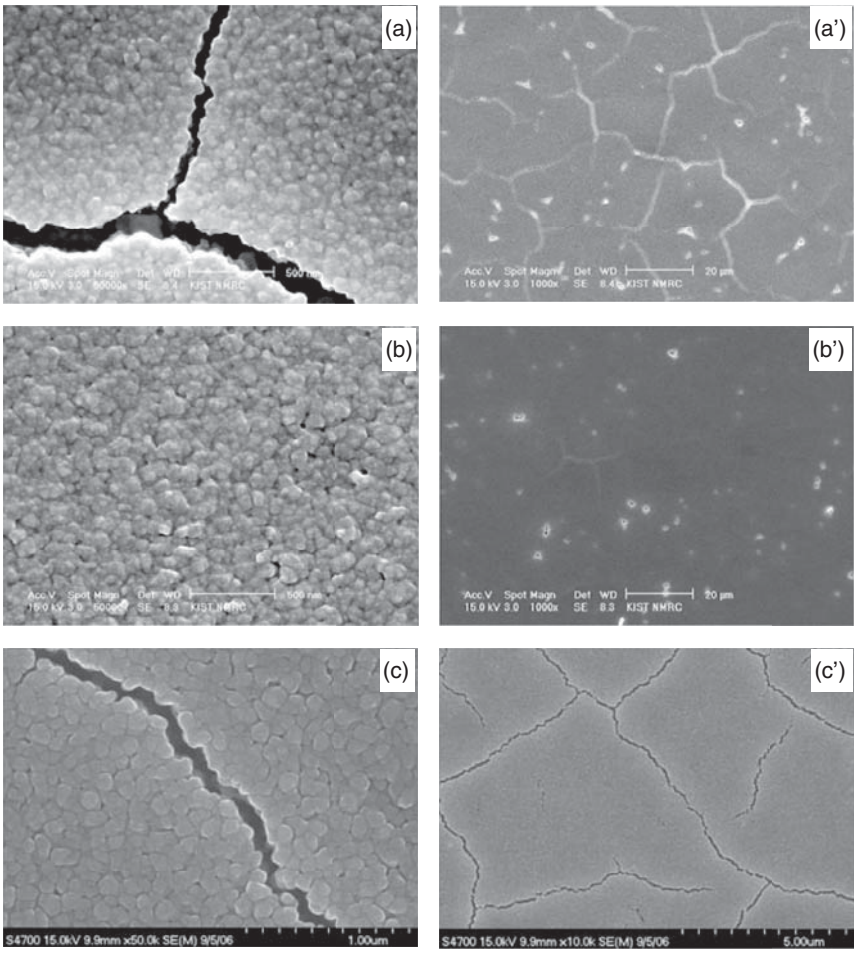

Figure 6. SEM images for $LiCoO_2$ thin film surfaces deposited at second step heat treatment conditions; (a),(a′) deposition at RT and RTA for 10min(×50,000, ×1,000), (b),(b′) deposition at 300°C and RTA for 10min (×50,000, ×1,000), (c),(c′) deposition at 600°C and RTA for 10min (×50,000, ×10,000).

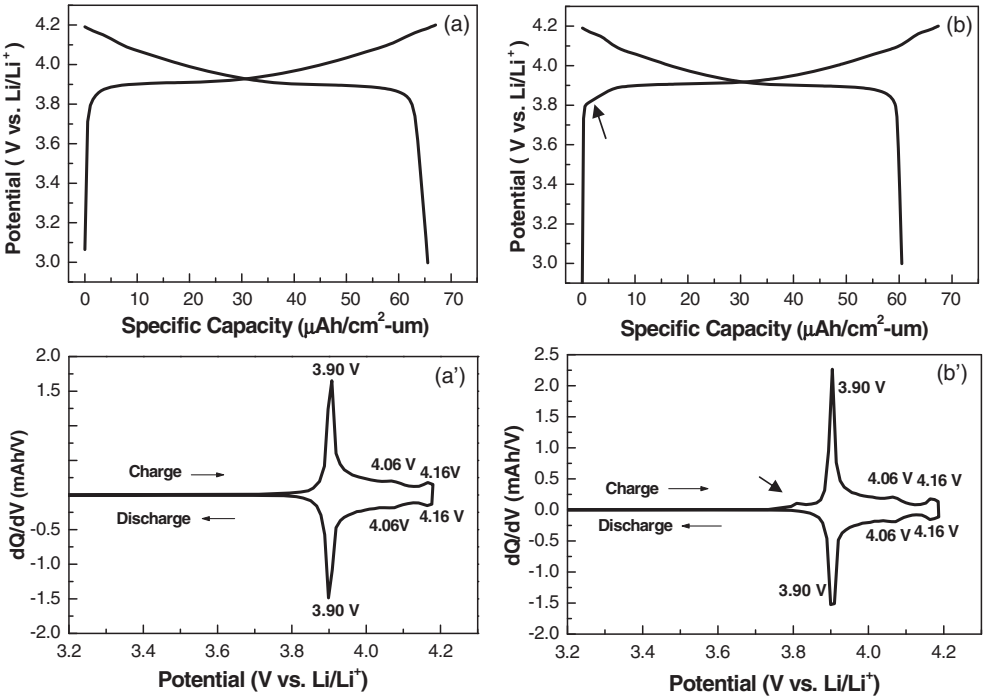

Figure 7. Charge-discharge and dQ/dV curves of $LiCoO_2$ thin film in half cell test: (a),(a′) deposition at 300°C and RTA for 10min and (b),(b′) deposition at 600°C and RTA for 10min.

70 nm–180 nm widths were observed in the as-deposited film at RT and when using RTA at 650°C for 10 min, and its shape was uniformly distributed over the film surface (Fig. 6a′ and 6b′). In contrast, the grain size slightly increased, and no cracks were observed in the film deposited at 300°C with RTA for 10 min (Figs. 6b, while cracks of 100 nm widths existed in the film deposited at 600°C with RTA (Figs. 6c and 6c′). Assuming that the thermal stress is the same during the RTA process, this stress may be contributing to reduced intrinsic or growth stress through substrate heating during deposition. When the RTA process was conducted directly on the $LiCoO_2$ thin film deposited at RT, the thermal energy was concentrated on the surface of the cathode film within a very short time and was gradually transferred to the inner structure, including the substrate and current collector, resulting in crystallization and densification of the $LiCoO_2$ thin film. However, residual stress was released in the form of cracks during cooling, with structural instability resulting from the different thermal expansion coefficients of the layers. Thus, the total film stress (σ_T) was decreasing. In the case of substrate heating at 600°C, the thermal energy during deposition can affect the film densification through atomic rearrangement of Li, Co and O and also partially contribute to the transformation from the LT to the HT phase of $LiCoO_2$ thin film. However, the energy can also cause small cracks induced by substrate stress, as shown in Fig. 2a′. For the additional crystallization at 650°C during the RTA process, the residual stress increases crack formation and also grain growth (Fig. 6c). Alternatively, the residual stress was insufficient to cause cracks in the film deposited at 300°C and mainly affected the atomic rearrangement. Therefore, structural stability is achieved in the first stage, and additional thermal energy caused by the RTA process primary contributes to film crystallization and grain growth as shown in the SEM image of Fig. 6b. The charge/discharge and dQ/dV curves of $LiCoO_2$ thin films treated using RTA after 300°C and 600°C deposition were demonstrated using a half-cell through the application of a current density of 48 $\mu A/cm^2$. As shown in Fig. 7a and 7b, the potential plateau region near 3.9 V was observed, and the specific capacity also increased significantly from 9.5 $\mu Ah/cm^2$-μm and 27 $\mu Ah/cm^2$-μm to 65 $\mu Ah/cm^2$-μm and 60 $\mu Ah/cm^2$-μm, respectively. The dQ/dV potential plateau peaks at 3.9 V, 4.06 V and 4.16 V during charging, corresponded to the same potentials during

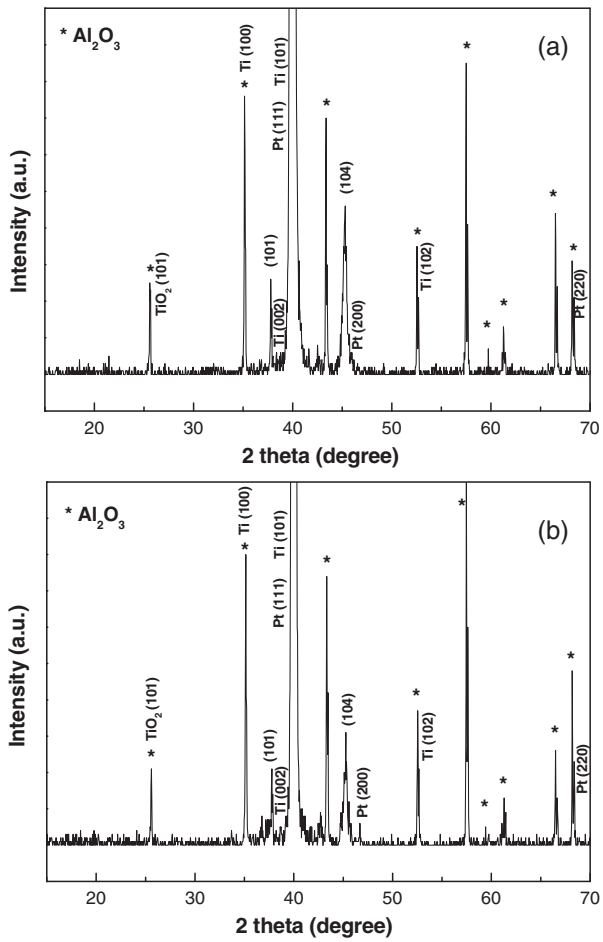

Figure 8. X-ray diffraction patterns of $LiCoO_2$ thin films: (a) deposition at 300°C and RTA for 10 min, and (b) deposition at 600°C and RTA for 10 min.

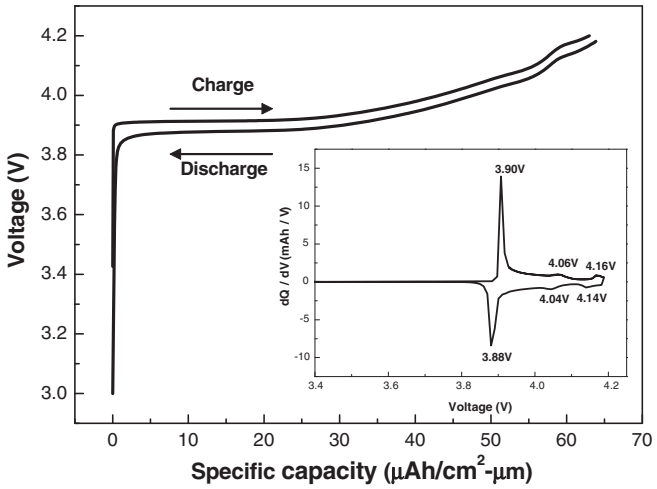

Figure 9. Charge-discharge and dQ/dV curves of Li/Lipon/crack free $LiCoO_2$ structured full cell after 300°C during deposition and RTA process.

discharging (Figs. 7a′ and 7b′). It is notable that superior reversibility without dQ/dV peak separation was observed. The weak peak near 3.8 V during the first charging process at 600°C with subsequent RTA was estimated to be due to a side reaction caused by a heterogeneous composition in the local region of $LiCoO_2$ through excess heat treatment. The main peak at 3.9 V was a primary phase transition between two rhombohedral structures, and the two small peaks at 4.06 V and 4.16 V were defined as phase transitions of order/disorder or hexagonal/monoclinic arrangements of the lithium ions.[28,29] Specifically, the phase transition of the hexagonal to monoclinic occurs during charging, and the inverse transition occurs during discharging. Figure 8 shows the XRD patterns of $LiCoO_2$ thin film treated with RTA after deposition at 300°C and 600°C. Most of the peaks were attributed to Al_2O_3 substrate, with some overlapping peaks from the lower layers. However, the preferred orientation peaks of (101) and (104) diffraction in the $LiCoO_2$ thin films were well developed in both conditions, although peak separation of the (006) and (012) planes near 38° and the (018) and (110) planes near 65° was not identified, which were usually observed as a HT phase. Additionally, the (003) peak disappeared. Thus, a crystal structure favorable for fast lithium intercalation/deintercalation was obtained through the two-step heat treatment process. An all-solid-state thin film battery was prepared using the Lipon solid electrolyte with crack-free $LiCoO_2$ thin film treated with RTA after 300°C deposition, and the charge/discharge and dQ/dV curves at a 1C rate were investigated, as shown in Fig. 9. Similar to the results of Fig. 7, the long potential plateau near 3.9 V corresponding to the primary phase transition in two hexagonal structures was observed, as well as the redox couples of 4.16 V / 4.06 V and 4.14 V / 4.04 V. The peak separation of 0.02 V in the dQ/dV curve was likely due to the internal resistance of the Lipon solid electrolyte. The two-step heat treatment is very effective for fabricating crack-free $LiCoO_2$ cathode thin films with a specific discharge capacity of 63.5 μAh/cm²-μm, corresponding to 92% of the theoretical value. Figure 10 shows the cycling performance of the Li/Lipon/crack-free $LiCoO_2$ structured cell (RTA after 300°C deposition). The first specific discharge capacity of 60 μAh/cm²-μm corresponded to 87% of the theoretical capacity, even at a 5 C rate (current density of 242 μAh/cm²), and capacity decay was negligible after 500 cycles. Additionally, excellent Coulombic efficiency of approximately 99.9% was observed.

Conclusions

The LT and HT mixed crystalline phase was obtained via substrate heating during sputtering; however, a two-step heat treatment was conducted using an additional RTA process within a very short time for excellent cell performance. In a first substrate heating step during sputtering, the average deposition rate linearly decreased as the substrate temperature increased; however, the atomic ratio of Li/Co was close to theoretical stoichiometry. Additionally, the substrate heating affected the texturing of the (003), (104) and (108) planes. When the RTA process was applied as a second step for the preferred orientation of the $LiCoO_2$ thin film, severe cracks of 70 nm - 180 nm and an approximately 100 nm width were observed in the as-deposited film at RT and 600°C, respectively. However, a crack-free $LiCoO_2$ thin film surface was deposited at 300°C. A half-cell test demonstrated a higher specific discharge capacity close to the theoretical value and good reversibility at both conditions. In an all-solid-state structure of Li/Lipon/crack-free $LiCoO_2$ with RTA after 300°C deposition, a specific discharge capacity of 60 μAh/cm²-μm at a 5 C rate and superior

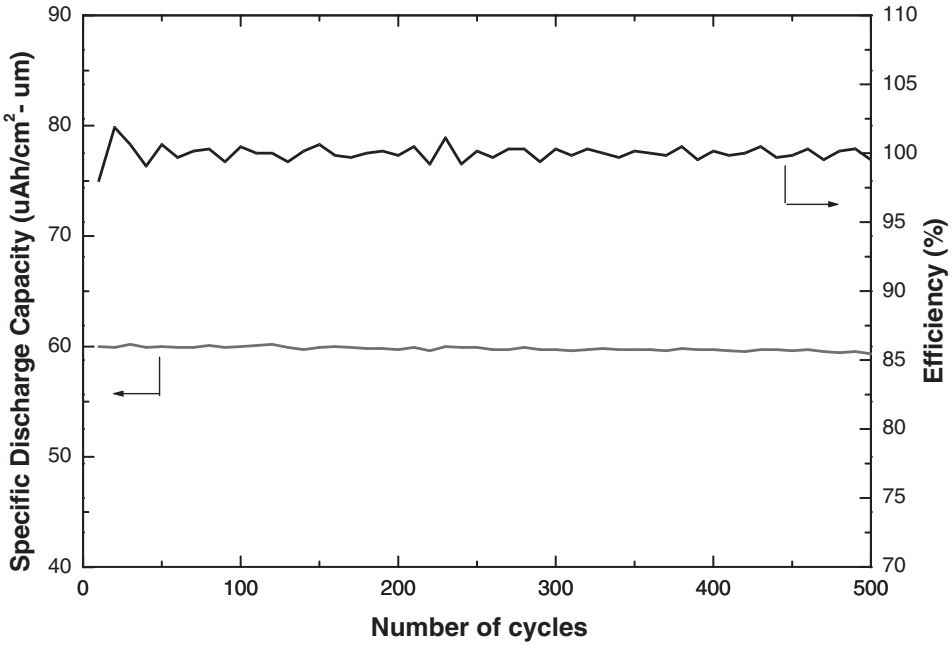

Figure 10. Specific discharge capacity and efficiency with cycling of Li/Lipon/crack free $LiCoO_2$ structured full cell at a 5 C rate with 300°C and RTA process condition.

cycling performance over 500 cycles were observed without capacity degradation.

Acknowledgments

This research was supported by the dual-use technology program of Korea ministry of national defense and also supported by the pioneer research center program through the national research foundation of Korea funded by the ministry of education, science and technology (2010-0019313).

References

1. A. Levasseur, M. Menetrier, R. Dormoy, and G. Meunier, *Mater. Sci. Eng*., **B3**, 5 (1989).
2. J. B. Bates, G. R. Gruzalski, N. J. Dudney, C. F. Luck, X.-H. Yu, and S. D. Jones, *Solid State Technol*., **36**, 59 (1993).
3. S. D. Johns and J. R. Akridge, *J. Power Sources*, **44**, 505 (1993).
4. J. B. Bates, G. R. Gruzalski, N. J. Dudney, C. F. Luck, and X. Yu, *Solid State Ionics*, **70&71**, 619 (1994).
5. N. J. Dudney, J. B. Bates, and B. J. Neudecker, *Encyclopedia of Materials: Science and Technology*, Elsevier Science, Section 6.9, Article 32 (2001).
6. B. Wang, J. B. bates, F. X. Hart, B. C. Sales, R. A. Zuhr, and J. D. Robertson, *J. Electrochem. Soc*., **143**, 3203 (1996).
7. J. B. Bates, N. J. Dudney, B. J. Neudecker, F. X. Hart, H. P. Jun, and S. A. Hackney, *J. Electrochem. Soc*., **147**, 59 (2000).
8. Y. I. Jang, B. J. Neudecker, and J. J. Dudney, *Electrochem. Solid State Lett*., **4**, A74 (2001).
9. Y. I. Jang, N. J. Dudney, D. A. Blom, and L. F. Allard, *J. Power Sources*, **119–121**, 295 (2003).
10. J. S. Van Sluytman, W. C. West, J. F. Whitacre, F. M. Alamgir, and S. G. Green-baum, *Electochim. Acta*, **51**, 3001 (2006).
11. S. W. Jeon, J. K. Lim, S. H. Lim, and S. M. Lee, *Electrochim.Acta*, **51**, 268 (2005).
12. M. Hayashi, M. Takahashi, and T. Shodai, *J. Power Sources*, **189**, 416 (2009).
13. H. Xia, L. Lu, and G. Ceder, *J. Alloys Compd*., **417**, 304 (2006).
14. P. Fragnaud, T. Brousse, and D. M. Schleich, *J. Power Sources*, **63**, 187 (1996).
15. H. Y. Park, S. R. Lee, Y. J. Lee, B. W. Cho, and W. I. Cho, *Mat. Chem. and Phys*., **93**, 70 (2005).
16. H. Y. Park, S. C. Nam, Y. C. Lim, K. G. Choi, K. C. Lee, G. B. Park, J. B. Kim, H. P. Kim, and S. B. Cho, *Electrochim. Acta*, **52**, 2062 (2007).
17. H. Y. Park, S. C. Nam, Y. C. Lim, K. G. Choi, K. C. Lee, G. B. Park, H. P. Kim, and S. B. Cho, *Korean J. Chem. Eng*., **23**, 832 (2006).
18. C. L. Liao and K. Z. Fung, *J Power Sources*, **128**, 263 (2004).
19. H. L. Chen, Y. M. Lu, and W. S. Hwang, *Surf & Coat Technol*., **198**, 138 (2005).
20. C. Ziebert, B. Ketterer, M. Rinke, C. Adelhelm, S. Ulrich, K. H. ZumGahr, S. Indris, and T. Schimmel, *Surf. & Coat. Technol*., **205**, 1589 (2010).
21. J. Prachařová, J. Přidal, J. Bludská, I. Jakubec, V. Vorlíček, Z. Máiková, Th. Dikonimos Makris, R. Giorgi, and L. Jastrabík, *J. Power Sources*, **108**, 204 (2002).
22. Y. Iriyama, M. Inaba, T. Abe, and Z. Ogumi, *J. Power Sources*, **94**, 175 (2001).
23. J. Pelleg, L. Z. Zevin, S. Lungo, and N. Croitoru, *Thin Solid Films*, **197**, 117 (1991).
24. F. X. Hart and J. B. Bates, *J. Appl. Phys*., **83**, 7560 (1998).
25. M. Antaya, K. Cearns, J. S. Preston, J. N. Reimers, and J. R. Dahn, *J. Appl. Phy.*, **76**, 2799 (1994).
26. R. J. Gummow and M. M. Thraceray, *Mat. Res. Bull*., **27**, 327 (1992).
27. S. G. Kang, S. Y. Kang, K. S. Ryu, and S. H. Chang, *Solid State Ionics*, **120**, 155 (1999).
28. J. N. Reimers and J. R. Dahn, *J. Electrochem. Soc*., **139**, 2091 (1992).
29. T. Ohzuku and A. Ueda, *J. Electrochem. Soc*., **141**, 2972 (1994).